Nonlinear statistical modeling and model discovery for cardiorespiratory data

D. G. Luchinsky,[1,2,3] M. M. Millonas,[2] V. N. Smelyanskiy,[2] A. Pershakova,[3] A. Stefanovska,[3,4] and P. V. E. McClintock[3]
[1]*Newstead Mission Critical Technologies, Inc., 9100 Wilshire Boulevard, Suite 540, East Beverly Hills, California 90212-3437, USA*
[2]*NASA Ames Research Center, Mail Stop 269-2, Moffett Field, California 94035, USA*
[3]*Department of Physics, Lancaster University, Lancaster LA1 4YB, UK*
[4]*Faculty of Electrical Engineering, University of Ljubljana, Tržaška 25, 1000 Ljubljana, Slovenia*
(Received 12 April 2005; published 19 August 2005)

We present a Bayesian dynamical inference method for characterizing cardiorespiratory (CR) dynamics in humans by inverse modeling from blood pressure time-series data. The technique is applicable to a broad range of stochastic dynamical models and can be implemented without severe computational demands. A simple nonlinear dynamical model is found that describes a measured blood pressure time series in the primary frequency band of the CR dynamics. The accuracy of the method is investigated using model-generated data with parameters close to the parameters inferred in the experiment. The connection of the inferred model to a well-known beat-to-beat model of the baroreflex is discussed.

DOI: 10.1103/PhysRevE.72.021905 PACS number(s): 87.19.Hh, 02.50.Tt, 05.10.Gg, 05.45.Tp

I. INTRODUCTION

Model identification is important for both fundamental and applied research [1–8] on the human cardiovascular system (CVS). Because of the complexity of CVS dynamics and the multiplicity of its mechanisms, it is inherently difficult or impossible to isolate and study individual response mechanisms in the intact organism [9]. In such cases mathematical models of cardiovascular control that are consistent with the experimental data can provide valuable insight [10,11]. Altered dynamics of the cardiovascular system is associated with a range of cardiovascular diseases and with increased mortality, and it is hoped that dynamical metrics will provide a means of evaluating autonomic activity and eventually form the basis for diagnostic tests for many conditions [12–16].

Notwithstanding that most cardiovascular controls are demonstrably nonlinear [8,10,13,17–20] and are perturbed by stochastic inputs [8,21,22], assumptions of model linearity [1,3–6,23,24] and/or determinism [10,17] are often made in an attempt to facilitate progress in cardiovascular system identification. Such choices are often influenced more by the ready availability of particular statistical tools and methodologies than by biophysical or medical considerations. It is therefore highly desirable to develop reliable methods of system identification that are free of such limitations and are capable of treating more realistic models. The latter could be used to relate difficult-to-access parameters to noninvasively measured data [11].

Thus, although a number of numerical schemes have been proposed recently to deal with different aspects of the inverse problem using linear approximations [1,5,25,26], or estimation of either the strength of some of the nonlinear terms [27,28] or the directionality of coupling [29–31], inverse cardiovascular problems remain difficult because of the complexity and nonlinearity of the cardiovascular interactions. The stochasticity of many dynamical inputs to the system presents an additional complication. The problem of nonlinear cardiovascular system identification has been addressed in a number of publications [7,8,32–35]. Nonlinearities generally require the use of more complex and involved numerical techniques [36–42], while the presence of dynamical noise in continuous systems can introduce systematic errors in the estimation of the model parameters [43,44]. Analogous difficulties arise in a broad range of scientific disciplines, including problems in lasers [45] and molecular motors [46], in epidemiology [47], and in coupled matter-radiation systems in astrophysics [48]. An obstacle to progress in these fields is the lack of general methods of dynamical inference for stochastic nonlinear systems. Accordingly, the methods described in this paper should be of broad interdisciplinary interest.

Following a short report published elsewhere [49], we now provide a full description of our method, applying it to the analysis of cardiorespiratory dynamics and doing so within a general nonlinear Bayesian framework for the inference of stochastic dynamical systems [44]. The basic methodology is described in Sec. II. The Bayesian inference scheme is outlined in Sec. III, and the technique is applied to the analysis of a univariate blood pressure (BP) time-series in Sec. IV. In this way, a simple nonlinear dynamical model based on coupled nonlinear oscillators [13,50,51] is found, able to describe time-series data in the relevant frequency range. In Sec. V, the accuracy of the method is investigated using model time-series data with parameters inferred from the experimental data. The results are considered in Sec. VI including a discussion of the connections between this model and the well-known beat-to-beat model of the baroreflex. Finally, Sec. VII summarizes the conclusions that can be drawn.

II. METHODOLGY

Our methodological framework involves three essential steps: (i) the input data are prepared; (ii) a parametrized class of models is chosen, with the hope that one of them may describe the data; and (iii) the parameters of this model class are inferred from the time-series data.

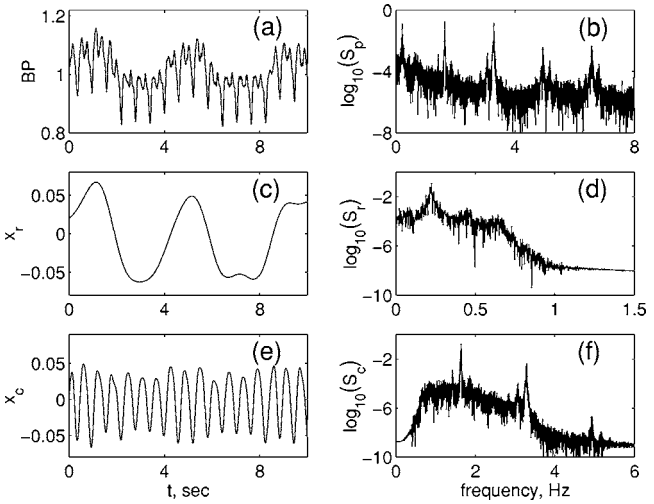

FIG. 1. Data derived from time-series record 24 of the MGH/MF Waveform Database available at www.physionet.org, before and after preprocessing. (a) Original time series of the central venous blood pressure and (b) its power spectrum. (c) Respiratory component produced by filtering the blood pressure time series with a 0.02 Hz, first-order, zero-phase, high-pass Butterworth filter and a 0.6 Hz, fifth order, zero-phase low-pass Butterworth filter and (d) its power spectrum. (e) Cardiac component produced by filtering the blood pressure time series with a 0.8–3.0 Hz, fourth-order, zero-phase, band-pass Butterworth filter and (d) its power spectrum. The chosen frequency ranges of the components were selected according to the criteria discussed in the text.

A. Data

We analyze a particular recording of the central venous blood pressure, a sample of which is shown in Fig. 1(a). A feature of this BP time-series is the presence of the two oscillatory components at frequencies approximately $f_r \approx 0.2$ Hz and $f_c \approx 1.7$ Hz (see spectrum of this signal shown in the Fig. 1) corresponding, respectively, to respiratory and cardiac oscillations. The effect of nonlinear terms, including those related to the nonlinear cardiorespiratory interaction (corresponding to the side peaks), are clearly evident. We note that the relative intensities and positions of the cardiac and respiratory components vary from subject to subject, with the average frequency of respiration being ~ 0.3 Hz and that of the heart beat being ~ 1.1 Hz.

In preprocessing cardiovascular data for model identification one has to bear in mind that CVS power spectra reflect a variety of complex cardiovascular interactions that give rise to peaks and other features over a broad frequency range [21,52–54]. In order to make sense of these multiscale phenomena, parametric modeling is usually restricted to a specific part of the power spectrum. It is clear that, in order to model the cardiorespiratory interaction, the frequency range considered must include at least the basic frequencies of cardiac and respiratory oscillations f_c and f_r and their combinational frequencies. Moreover, as was pointed out earlier [55,56] locally measured blood pressure signals resemble a steady-state oscillation and the sum of the first three harmonics contains more then 70% of the total signal variance. Therefore, it is desirable that at least the second and the third harmonics (see also discussion below), besides the basic frequencies of the respiratory and cardiac oscillations, are included in the frequency range of modeling.

B. Models

When one considers modeling the cardiovascular system, one usually envisages the construction of a model based on biophysical principles, one that is capable of generating solutions that reproduce, to some degree, the measured data. This approach tackles the *forward modeling* problem [10,17,22,57]. One may also consider the *inverse modeling* problem in which models are built specifically to describe measured data [1,3–5,35]. Both approaches have proven useful in the context of cardiovascular research, with the forward approach providing valuable insight into the system and its causal relationships, and the inverse approach providing a useful means of intelligent monitoring of cardiovascular function in patients.

As a third alternative one may try to bridge the two approaches by building a model that accurately reproduces the experimental observations while at the same time being based on the physiological principles of circulation. In such a case the form of the mathematical model is taken from physiological principles, with its component parts corresponding, to a greater or lesser degree, to specific physiological mechanisms, while the values of some or all of the parameters of the mathematical model are inferred directly from the data. In such a case it is hoped that information with direct physiological significance, more than mere mathematical or statistical characterization, can be inferred from the data.

Many studies have been carried out to explore the physiological mechanisms underlying cardiorespiratory interactions [58–60]. Those shown to be involved are the modulation of cardiac filling pressure by respiratory movements [61], the direct respiratory modulation of parasympathetic and sympathetic neural activity in the brain stem [62], and the respiratory modulation of baroreceptor feedback control [63]. A common feature that these mechanisms is that they are nonlinear, have a dynamical (or memory) component, and are subject to exogenous fluctuations [7,13,50,64–67].

A simple beat-to-beat model was introduced by DeBoer *et al.*[57,68] to describe the cardiorespiratory system. The model has further been elaborated recently in [10,11,22]. Insight into cardiorespiratory dynamics can also be gained through inverse modeling, treating the cardiac and respiratory cycles as coupled nonlinear oscillators [13,21,50–52]. In this approach spectral and synchronization features [32–34] observed in the time-series data are interpreted, physiologically, and related to the model parameters [13]. However, the model parameters could not be identified directly from the time-series data. Instead, they were deduced on the basis of physiological assumptions and then evaluated through extensive computer simulations [21].

The simplest model that can reproduce steady-state oscillations of the blood pressure signal at two fundamental frequencies is a system of two coupled limit cycles on a plane. The Poincaré-Bendixson theory of planar dynamical systems

implies that, for a system to have a limit cycle in a simply connected region, the divergence of the vector field must change sign within this region [69]. We conclude, therefore, that the simplest system that can reproduce the BP signal features considered is a planar one with limit cycles whose vector field contains polynomials of order 3. Accordingly, we model the time-series data as a system of two coupled oscillators with vector fields including nonlinearities (as well as those in coupling terms) up to the third order in the form

$$\dot{x}_r = a_1 x_r + b_1 y_r, \quad \dot{y}_r = \sum_{i=1}^{N} \alpha_i \phi_i(\mathbf{x},\mathbf{y}) + \sum_{j=1}^{2} \sigma_{1j}\xi_j, \qquad (1)$$

$$\dot{x}_c = a_2 x_c + b_2 y_c, \quad \dot{y}_c = \sum_{i=1}^{N} \beta_i \phi_i(\mathbf{x},\mathbf{y}) + \sum_{j=1}^{2} \sigma_{2j}\xi_j,$$

$$\langle \xi_i(t) \rangle = 0, \quad \langle \xi_i(t)\xi_j(t') \rangle = \delta_{ij}\delta(t-t'). \qquad (2)$$

Here the noise matrix σ mixes zero-mean white Gaussian noises $\xi_j(t)$, which are related to the diffusion matrix $D = \sigma\sigma^T$. The base functions are chosen in the form

$$\phi = \{1, x_r, x_c, y_r, y_c, x_r^2, x_c^2, y_r^2, y_c^2, x_r y_r, x_c y_c, x_r^3, x_c^3, x_r^2 y_r, x_c^2 y_c, x_r y_r^2, x_c y_c^2, y_r^3, y_c^3, x_r x_c, x_r^2 x_c, x_r x_c^2\}. \qquad (3)$$

Signals x_r and x_c can be directly related to the respiratory and cardiac components of the blood pressure signal shown in the Figs. 1(c) and 1(e) (see also Sec. IV for a more detailed discussion). The restrictions imposed on the equations for $\dot{x}_r$ and $\dot{x}_c$ in (1) and (2) are determined mainly by the fact that we have to infer four unknown dynamical variables using univariate time-series data (see Sec. III for further details). The parametric representation of (1) and (2) covers a wide range of models with limit cycles in the plane. In particular, with appropriate choices of model parameters it can describe either a van der Pol or a FitzHugh-Nagumo (FHN) oscillator system, both of which have been widely used in the context of cardiovascular modeling. Furthermore, the choice of the parametric model in the form of (1) and (2) allows one to relate them to physiological parameters characterizing the autonomous nervous system (note discussion in Sec. VI). See [13] for an alternative choice and corresponding physiological reasoning, taking account of more complex interactions and considering the influence of blood flow and pressure propagation through the closed system of vessels.

C. Parameters

Following the logic of the inverse modeling approach, we must then identify the parameters $\mathcal{M} = \{\mathbf{a}, \mathbf{b}, \boldsymbol{\alpha}, \boldsymbol{\beta}, D\}$ of the model (1) and (2) that reproduce the dynamical and spectral features of the BP signal shown in the Fig. 1. Terms representing nonlinear cardiorespiratory interactions are described by the last three base functions in (3). The correspondence of these terms to the experimentally observed combinational frequencies in the BP signal is summarized in the Fig. 2. It can be seen from the figure that the same combinational frequencies correspond to the nonlinear coupling terms in both limit-cycle systems in the model. A *nonlinear* time-series analysis is therefore a requirement for the identification of such a model.

III. BAYESIAN INFERENCE OF STOCHASTIC NONLINEAR DYNAMICAL MODELS

Details of the Bayesian technique can be found elsewhere [44], but, for completeness, we now provide a brief description of the main steps of the algorithm.

Stochastic nonlinear dynamical models of the type (1) and (2) can be expressed as a multidimensional nonlinear Langevin equation

$$\dot{\mathbf{x}}(t) = \mathbf{f}(\mathbf{x}) + \varepsilon(t) = \mathbf{f}(\mathbf{x}) + \sigma\xi(t), \qquad (4)$$

where $\varepsilon(t)$ is an additive stationary white, Gaussian vector noise process characterized by

$$\langle \xi(t) \rangle = 0, \quad \langle \xi(t)\xi^T(t') \rangle = \hat{\mathbf{D}}\delta(t-t'), \qquad (5)$$

where $\hat{\mathbf{D}}$ is a diffusion matrix.

It is assumed that the trajectory $x(t)$ of this system is observed at sequential time instants $\{t_k; k = 0, 1, \ldots, K\}$ so that the time series $\mathcal{S} = \{s_k \equiv s(t_k)\}$ thus obtained is related to the (unknown) "true" system states $\mathcal{X} = \{x_k \equiv x(t_k)\}$ through some conditional probability density function (PDF) $p_o(\mathcal{S}|\mathcal{X})$.

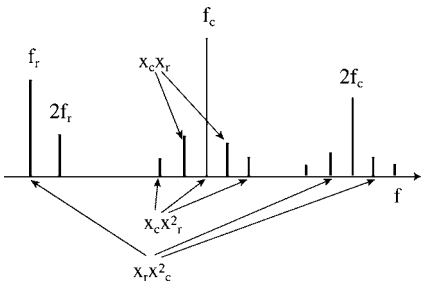

FIG. 2. Summary of the main harmonics of the cardiac and respiratory components observed in the BP signal. The correspondences between the nonlinear terms of the model [Eqs. (1) and (2)], and the frequencies observed in the time-series data are shown by arrows.

The *a priori* expert knowledge about the model parameters, if any, is summarized in the so-called prior PDF $p_{\rm pr}(\mathcal{M})$. In our case we chose the prior PDF in the form of a zero-mean Gaussian distribution for the model parameters and uniform distributions for the coefficients of the diffusion matrix.

If experimental time-series data $\mathcal{S}$ are available, they can be used to improve the estimation of the model parameters. The improved knowledge of the models parameters is summarized in the *posterior* conditional PDF $p_{\rm post}(\mathcal{M}|\mathcal{S})$, which is related to the prior PDF via Bayes' theorem

$$p_{\rm post}(\mathcal{M}|\mathcal{S}) = \frac{\ell(\mathcal{S}|\mathcal{M})p_{\rm pr}(\mathcal{M})}{\int \ell(\mathcal{S}|\mathcal{M})p_{\rm pr}(\mathcal{M})\mathrm{d}\mathcal{M}}. \tag{6}$$

Here, $\ell(\mathcal{S}|\mathcal{M})$, usually termed the *likelihood*, is the conditional PDF that relates measurements $\mathcal{S}$ to the dynamical model. The denominator on the right-hand side of (6) is a normalizing factor. In practice, (6) can be applied iteratively using a sequence of data blocks $\mathcal{S},\mathcal{S}'$, etc. The posterior PDF computed from block $\mathcal{S}$ serves as the prior PDF for the next block $\mathcal{S}'$, etc. For a sufficiently large number of observations, $p_{\rm post}(\mathcal{M}|\mathcal{S},\mathcal{S}',\ldots)$ becomes sharply peaked at a certain most probable model $\mathcal{M}=\mathcal{M}^*$.

The main efforts in research on stochastic nonlinear dynamical inference are focused on construction of the likelihood function, which compensates noise-induced errors, and on the introduction of efficient algorithms for optimization of the likelihood function and integration of the normalization factor (cf. [36,37,43,70]).

In our earlier work [44] a technique of nonlinear dynamical inference of stochastic systems was presented that solves both problems. To avoid extensive numerical methods of optimization of the likelihood function and integration of the normalization factor, we suggested parametrization of the vector field of (4) in the form

$$\mathbf{f}(\mathbf{x}) = \hat{\mathbf{U}}(\mathbf{x})\mathbf{c} \equiv \mathbf{f}(\mathbf{x};\mathbf{c}), \tag{7}$$

where $\hat{\mathbf{U}}(\mathbf{x})$ is a $N\times M$ matrix of suitably chosen basis functions $\{U_{nm}(\mathbf{x});n=1:N,m=1:M\}$, and $\mathbf{c}$ is an M-dimensional coefficient vector. An important feature of (7) is that, while possibly highly nonlinear in $\mathbf{x}$, $\mathbf{f}(\mathbf{x};\mathbf{c})$ is strictly linear in $\mathbf{c}$.

The computation of the likelihood function can be cast in the form of a path integral over the random trajectories of the system [71,72]. Using the uniform sampling scheme introduced above we can write the logarithm of the likelihood function in the following form for a sufficiently small time step h (cf. [71,72]):

$$\begin{aligned} -\frac{2}{K}\log \ell(\mathbf{y}|\mathcal{M}) &= \ln\det\hat{\mathbf{D}} + \frac{h}{K}\sum_{k=0}^{K-1}[\mathbf{v}(\mathbf{y}_k)\mathbf{c} + (\dot{\mathbf{y}}_k - \hat{\mathbf{U}}_k\mathbf{c})^T\hat{\mathbf{D}}^{-1}(\dot{\mathbf{y}}_k - \hat{\mathbf{U}}_k\mathbf{c})] \\ &\quad + N\ln(2\pi h), \end{aligned} \tag{8}$$

which relates the dynamical variables $\mathbf{x}(t)$ of the system (4) to the observations $\mathbf{s}(t)$. Here, we introduce the following notation: $\hat{\mathbf{U}}_k \equiv \hat{\mathbf{U}}(\mathbf{y}_k)$; $\dot{\mathbf{y}}_k \equiv h^{-1}(\mathbf{y}_{k+1}-\mathbf{y}_k)$; and vector $\mathbf{v}(\mathbf{x})$ with components

$$\mathrm{v}_m(\mathbf{x}) = \sum_{n=1}^{N}\frac{\partial U_{nm}(\mathbf{x})}{\partial x_n}, \quad m=1{:}M.$$

The vector elements $\{c_m\}$ and the matrix elements $\{D_{nn'}\}$ together constitute a set $\mathcal{M}=\{\mathbf{c},\hat{\mathbf{D}}\}$ of unknown parameters to be inferred from the measurements $\mathcal{S}$.

Choosing the prior PDF in the form of Gaussian distribution

$$p_{\rm pr}(\mathcal{M}) = \sqrt{\frac{\det(\hat{\Sigma}_{\rm pr}^{-1})}{(2\pi)^M}}\exp\left(-\frac{1}{2}(\mathbf{c}-\mathbf{c}_{\rm pr})^T\hat{\Sigma}_{\rm pr}^{-1}(\mathbf{c}-\mathbf{c}_{\rm pr})\right) \tag{9}$$

and substituting $p_{\rm pr}(\mathcal{M})$ and the likelihood $\ell(\mathcal{S}|\mathcal{M})$ into (6) yields the posterior PDF $p_{\rm post}(\mathcal{M}|\mathcal{S})=\text{const}\times\exp[-L(\mathcal{M}|\mathcal{S})]$, where

$$L(\mathcal{M}|\mathcal{S}) \equiv L_{\mathbf{s}}(\mathbf{c},\hat{\mathbf{D}}) = \tfrac{1}{2}\rho_{\mathbf{s}}(\hat{\mathbf{D}}) - \mathbf{c}^T\mathbf{w}_{\mathbf{s}}(\hat{\mathbf{D}}) + \tfrac{1}{2}\mathbf{c}^T\hat{\boldsymbol{\Xi}}_{\mathbf{s}}(\hat{\mathbf{D}})\mathbf{c}. \tag{10}$$

Here, use was made of the definitions

$$\rho_{\mathbf{s}}(\hat{\mathbf{D}}) = h\sum_{k=0}^{K-1}\dot{\mathbf{s}}_k^T\hat{\mathbf{D}}^{-1}\dot{\mathbf{s}}_k + K\ln(\det\hat{\mathbf{D}}), \tag{11}$$

$$\mathbf{w}_{\mathbf{s}}(\hat{\mathbf{D}}) = \hat{\Sigma}_{\rm pr}^{-1}\mathbf{c}_{\rm pr} + h\sum_{k=0}^{K-1}\left[\hat{\mathbf{U}}_k^T\hat{\mathbf{D}}^{-1}\dot{\mathbf{s}}_k - \frac{\mathbf{v}(\mathbf{s}_k)}{2}\right], \tag{12}$$

$$\hat{\boldsymbol{\Xi}}_{\mathbf{s}}(\hat{\mathbf{D}}) = \hat{\Sigma}_{\rm pr}^{-1} + h\sum_{k=0}^{K-1}\hat{\mathbf{U}}_k^T\hat{\mathbf{D}}^{-1}\hat{\mathbf{U}}_k. \tag{13}$$

The mean values of $\mathbf{c}$ and $\hat{\mathbf{D}}$ in the posterior distribution give the best estimates for the model parameters for a given block of data $\mathcal{S}$ of length K and provide the global minimum of $L_{\mathbf{s}}(\mathbf{c},\hat{\mathbf{D}})$. We handle this optimization problem in the following way. Assume for the moment that $\mathbf{c}$ is known in (10). Then the posterior distribution over $\hat{\mathbf{D}}$ has a mean $\hat{\mathbf{D}}'_{\rm post}=\hat{\boldsymbol{\Theta}}_{\mathbf{s}}(\mathbf{c})$ that provides a minimum of $S_{\mathbf{s}}(\mathbf{c},\hat{\mathbf{D}})$ with respect to $\hat{\mathbf{D}}=\hat{\mathbf{D}}^T$. Its matrix elements are

$$\hat{\boldsymbol{\Theta}}_{\mathbf{s}}^{nn'}(\mathbf{c}) \equiv \frac{1}{K}\sum_{k=0}^{K-1}[\dot{\mathbf{s}}_k - \hat{\mathbf{U}}(\mathbf{s}_k)\mathbf{c}]_n[\dot{\mathbf{s}}_k - \hat{\mathbf{U}}(\mathbf{y}_k)\mathbf{c}]_{n'}^T. \tag{14}$$

Alternatively, assume next that $\hat{\mathbf{D}}$ is known and note from (10) that in this case the posterior distribution over $\mathbf{c}$ is Gaussian. Its covariance is given by $\hat{\boldsymbol{\Xi}}_{\mathbf{s}}(\hat{\mathbf{D}})$ and the mean $\mathbf{c}'_{\rm post}$ minimizes $L_{\mathbf{s}}(\mathbf{c},\hat{\mathbf{D}})$ with respect to $\mathbf{c}$

$$\mathbf{c}'_{\rm post} = \hat{\boldsymbol{\Xi}}_{\mathbf{s}}^{-1}(\hat{\mathbf{D}})\mathbf{w}_{\mathbf{s}}(\hat{\mathbf{D}}). \tag{15}$$

We repeat this two-step optimization procedure iteratively, starting from some prior values $\mathbf{c}_{\rm pr}$ and $\hat{\Sigma}_{\rm pr}$.

IV. ESTIMATION OF PARAMETERS OF CARDIORESPIRATORY INTERACTION FROM UNIVARIATE TIME-SERIES DATA

In order to apply algorithm (12)–(15) for the identification of the model of nonlinear cardiorespiratory dynamics (1) and (2) from the univariate BP time-series of the type shown in Fig. 1(a) we have to extract time-series data corresponding to the four dynamical variables in the model. Accordingly, we divide the total spectrum into a low-frequency respiratory component $s_r(t)$ and high-frequency cardiac component $s_c(t)$ as is shown in Figs. 1(c) and 1(e).

A discussion of the physiological relevance of this spectral separation can be found in [13,51]. However, it is perfectly correct to consider this separation to be a mathematical *ansatz*. The filter parameters (see Fig. 1) were chosen to preserve the second and third harmonics of these signals. The two dynamical variables of the model, $x_r(t)$ and $x_c(t)$ given by (1),(2), can be identified with the two-dimensional time series of observations $\mathbf{s}(t)=\{s_r(t),s_c(t)\}$ introduced above and can be interpreted as the contribution to blood pressure from cardiac and respiratory activity. The remaining two dynamical variables $\mathbf{y}(t)=\{y_r(t),y_c(t)\}$ can be related to the observations $\{\mathbf{s}(t_k)\}$ as follows:

$$b_n y_n(t_k) = \frac{s_n(t_k+h)-s_n(t_k)}{h} + a_n s_n(t_k), \tag{16}$$

where $n=r,c$. In this way we obtain the velocity of blood pressure changes contributed by the cardiac and respiratory components. The relation (16) is a special form of embedding. As mentioned above, it allows one to infer a wide class of dynamical models of the cardiorespiratory interactions, including FitzHugh-Nagumo oscillators. The reason that we introduced restrictions on the form of the first equations in (1),(2) is now clear; it is to reduce the number of embedding parameters that must be selected to minimize the cost (10) and provide the best fit to the measured time series $\{\mathbf{s}(t_k)\}$. The corresponding simplified model of the nonlinear interaction between the cardiac and respiratory limit cycles can now be written in a form corresponding to the parametrization (7), as follows:

$$\dot{\mathbf{y}} = \hat{\mathbf{U}}(\mathbf{s},\mathbf{y})\mathbf{c} + \boldsymbol{\xi}(t), \tag{17}$$

where $\boldsymbol{\xi}(t)$ is a two-dimensional Gaussian white noise with correlation matrix $\hat{\mathbf{D}}$ and the matrix $\hat{\mathbf{U}}$ will have the following block structure:

$$\hat{\mathbf{U}} = \left[\begin{pmatrix} \phi_1 & 0 \\ 0 & \phi_1 \end{pmatrix} \cdots \begin{pmatrix} \phi_2 & 0 \\ 0 & \phi_2 \end{pmatrix} \cdots \begin{pmatrix} \phi_B & 0 \\ 0 & \phi_B \end{pmatrix} \right]. \tag{18}$$

Here $B=22$; thus, there are 22 2×2 diagonal blocks formed by the basis functions given in (3) and the vector of unknown parameters $\mathbf{c}$ is of length $M=2B$.

Finally, the model (17),(18) has to be inferred using the method described in Sec. III. A comparison between the time series of the inferred and actual cardiac oscillations is shown in Fig. 3. Similar results are obtained for the respiratory oscillator, as shown in the Fig. 4. In each case, the level of agreement obtained is encouraging. The nonlinear coupling

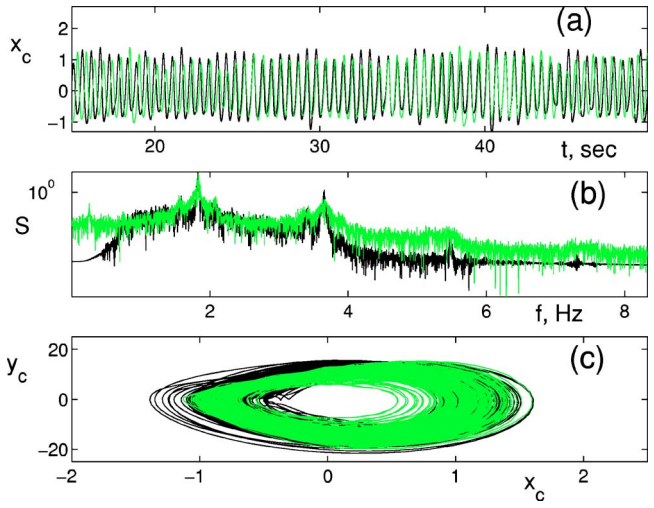

FIG. 3. (Color online) (a) Time series of the cardiac oscillations $x_c(t_n)=s_c(t_n)$ in arbitrary units (black line) obtained from measurements of the central venous blood pressure. The sampling rate was 90 Hz after resampling of the original signal. Inferred time series of the cardiac oscillator is shown by the green line. (b) Power spectra of cardiac oscillations obtained, respectively, from the real data (black line) and from the inferred oscillations (green line). (c) Limit cycles of the cardiac oscillations $x_c(n),y_c(n)$ obtained, respectively, from real data as described in the text (black line) and by inference (green line).

parameters and noise intensity of the cardiac oscillations have been estimated to have the following values: $\beta_{20}=2.2$, $\beta_{21}=0.27$, $\beta_{22}=-8.67$, and $\langle \xi_c^2(t)\rangle=8.13$. The parameters characterizing coupling of respiratory oscillations to the car-

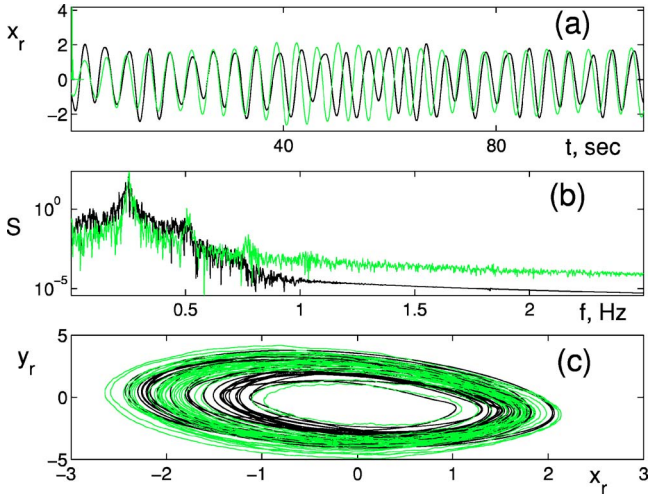

FIG. 4. (Color online) (a) Time series of the respiratory oscillations $x_r(t_n)=s_r(t_n)$ in arbitrary units (black line) obtained from measurements of central venous blood pressure. The sampling rate was 90 Hz after resampling of the original signal. Inferred time series of the respiratory oscillator is shown by the green line. (b) Power spectra of the respiratory oscillations obtained, respectively, from the real data (black line) and from the inferred oscillations (green line). (c) Limit cycles of the respiratory oscillations $x_r(n),y_r(n)$ obtained from real data as described in the text (black line) and from the inferred oscillations (green line).

diac oscillations were estimated as $\alpha_{20}=0.12$, $\alpha_{21}=0.048$, $\alpha_{22}=-0.066$, and $D_{11}=0.18$. Consistent with expectations, in all experiments the parameters of the nonlinear coupling are more than an order of magnitude higher for the cardiac oscillations as compared to their values for the respiratory oscillations, reflecting the fact that respiration strongly modulates cardiac oscillations, while the effect of the cardiac oscillations on respiration is relatively weak.

We have thus shown that this method enables one to simultaneously infer the relevant coupling strengths and noise parameters directly from a noninvasively measured time series. We view this demonstration of principle as one step toward the practical use of this technique for cardiorespiratory modeling and its potential for clinical applications. A number of very important physiological and mathematical issues arise in relation to the application of the technique to specific problems, and we hope to address some of these in future publications. Next, however, we consider, explicitly, the problem of estimating the accuracy of the method and initiate a discussion of the connections between the inferred parameters and the indices of autonomous cardiovascular control.

V. VALIDATION OF THE METHOD USING MODEL-GENERATED TIME-SERIES DATA

It is desirable to check the performance of the method on synthesized time-series data obtained by numerically simulating the model (1),(2) using parameters inferred from the CVS data. To this end we consider a model-generated signal $x(t)=x_r(t)+x_c(t)$ as the time-series data input $s(t)$ for the inference. Here $x_r(t)$, $x_c(t)$ are obtained from numerical simulations of the model (1),(2) with parameters inferred from the experimental BP signal described in Sec. IV.

First, we verify that the decomposition of the input signal $s(t)$ into low-frequency $\tilde{s}_r$ and high-frequency $\tilde{s}_c$ components allows one to reconstruct the original signal. The decomposition is effected using two bandpass Butterworth filters, which were followed by application of the embedding procedure (16). In Fig. 5 we compare the velocity of the respiratory component of the original signal $y_r(t)$ with the reconstructed velocity $\tilde{y}_r(t)$. The agreement is excellent. Similar results are obtained for the reconstruction of the high-frequency component. We note, in particular, that the noise introduced by embedding can be neglected because it is more than an order of magnitude smaller then the dynamical noise in the signal.

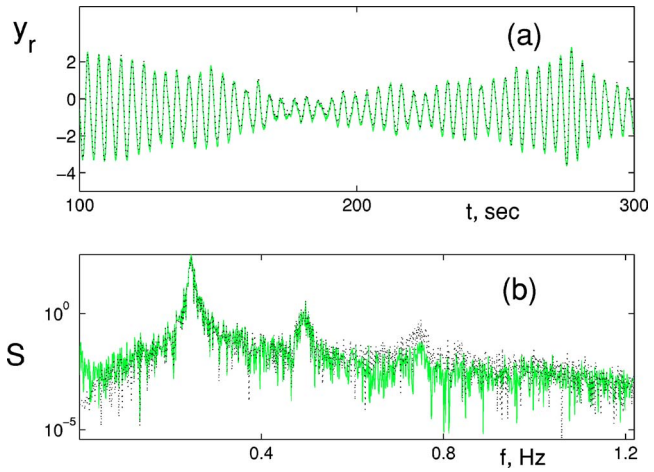

FIG. 5. (Color online) (a) Velocity of the respiratory oscillations of the original signal $y_r(t)$ (green line) is compared to the signal $\tilde{y}_r(t_k)$ (black dashed line) obtained as a result of filtration of $s(t)$ followed by the embedding $b_1\tilde{y}_r(t_k)=(s_r(t_k+h)-s_r(t_k))/h+a_2s_r(t_k)$. (b) Power spectra of the signals shown in (a), with the same color coding.

Now we can apply the inference procedure described in Sec. IV to estimate nonlinear coupling parameters of the model from the synthesized univariate time-series data. The results of the estimation are summarized in the Table I. It can be seen from the table that the method allows one to estimate the nonlinear coupling parameter, at least to the correct order of magnitude. For some parameters the estimation accuracy is much better, but in practice the correct values are not known.

Similar results are obtained for the estimation of other parameters of the model. Using parameter values estimated from the univariate model-generated data, one can reconstruct very closely the dynamical and spectral features of the original system as shown in the Fig. 6. The largest estimation errors are for the noise intensity, as shown in the last two columns of Table I. This result can be easily understood in that filtration of the signals has the strongest effect on the noise spectrum of the system. However, the filter-induced errors are systematic and thus can be corrected for based on tests with model-generated data.

The main source of error is related to the spectral decomposition of the univariate data, and it is therefore systematic.

TABLE I. Absolute values of the coefficients of nonlinear cardiorespiratory interactions corresponding to the last three base functions in (3), $\{x_rx_c, x_r^2x_c, x_rx_c^2\}$. The coefficient $\{\alpha_i\}$ corresponds to respiration coupling to the cardiac rhythm. Coefficients $\{\beta_i\}$ correspond to the cardiac oscillation coupling to respiration. For each set of coefficients the actual values (top row) are compared to the mean inferred values obtained from 100 nonoverlapped 1000 s blocks of data $x(t)=x_r(t)+x_c(t)$. Each block includes 50 000 points with a sampling time of 0.02 s (middle row). The estimation error is shown in the bottom line.

α_{20}	β_{20}	α_{21}	β_{21}	α_{22}	β_{22}	D_{11}	D_{22}
0.12	2.2	0.048	0.27	−0.066	−8.67	0.18	8.13
0.18	6.32	0.011	0.49	0.053	6.03	0.017	3.44
51.2%	186.8%	75.9%	102.7%	27.9%	30.6%	90.8%	57.7%

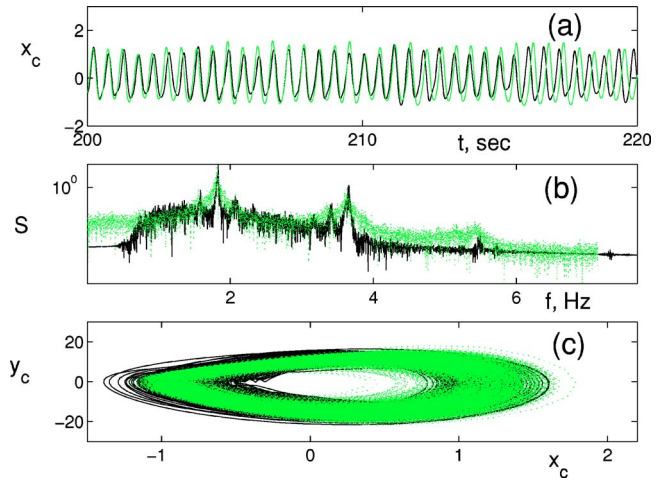

FIG. 6. (Color online) (a) Synthetically generated cardiac time series $x_c(t_n)$ in arbitrary units (black line) obtained from model (1),(2), compared to inferred time series of the cardiac oscillator (green line). (b) Power spectrum of the model-generated cardiac oscillations (black line) compared to that of the inferred oscillations (green dashed line). (c) Limit cycles of the model-generated respiratory oscillations $x_c(n), y_c(n)$ (black line) and of the inferred oscillations (green dashed line).

To illustrate this point we use the original synthesized time-series data $\{x_r(t), x_c(t), y_r(t), y_c(t)\}$ for two coupled oscillators to infer parameters of the model (1),(2). The results of inference of the coupling parameters are summarized in Table II. It can be seen that the values of the parameters can be estimated with relative error $<10\%$. In particular, the relative error of estimation of the noise intensity is now $<4\%$. The accuracy of the estimation can be further improved by increasing the total time of observation of the system dynamics as explained in [44].

These results should be compared to estimates of either relative strength of some of the nonlinear terms [27] or the directionality of coupling [29,30] from bivariate time-series data. It becomes clear that our algorithm provides an alternative effective approach to the analysis of cardiovascular coupling. In particular, the results of this section validate the application of the method to the measured cardiovascular data and demonstrate that it is indeed possible to simultaneously estimate the strength, directionality, and noise of nonlinear cardiorespiratory coupling form the univariate blood pressure signal.

VI. DISCUSSION

It is important to establish a relationship between the model parameters and physiological parameters of the cardiovascular system. A beat-to-beat model describing the relationships between blood pressure and respiration in simple but physiologically meaningful terms is that due to DeBoer *et al.* [57,68]. The DeBoer model incorporates several well-known physiological laws of the cardiorespiratory system based on static relationships. Recent extensions and modifications of this model have included [10,11,22]. The problem of inverse modeling was not addressed in this earlier work, and it is therefore very desirable to connect it to the approach presented here.

The DeBoer model describes the beat-to-beat evolution of the state variables shown in the Fig. 7(a): systolic pressure (S), diastolic pressure (D), RR intervals (I), and arterial decay time ($T=R\times C=$peripheral resistance$\times$arterial compliance). Following the brief account of the DeBoer model given in [17] and neglecting for the sake of simplicity variations in the peripheral resistance, we can write the corresponding set of difference equations as

$$D_i = S_{i-1}\exp[(-2/3)I_{i-1}/T], \tag{19}$$

$$S_i = D_i + \gamma I_{i-1} + C_1 + A\sin(2\pi f t), \tag{20}$$

$$I_i = G_v S'_{i-\tau_v} + G_\beta F(S', \tau_\beta) + C_2. \tag{21}$$

Here C_1, C_2, and C_3 are constants, and the sigmoidal nature of the baroreceptor sensitivity is accounted for by defining an effective systolic pressure (S') [57]

$$S'_i = S_0 + 18\arctan\frac{(S-S_0)}{18}. \tag{22}$$

The first equation (19) follows from the Windkessel model of the circulation, whereas the second equation (20) expresses the contractile properties of the myocardium in accordance with Starling's law, which takes into account the mechanical effect of circulation on the BP [55,57]. The last equation (21) includes, explicitly, two mechanisms of cardiovascular control defined by their respective gain (G) and delay (τ): (i) the fast vagal control of the heart rate $G_v S'_{i-\tau_v}$, and (ii) the slower β-sympathetic control of the heart rate $G_\beta F(S', \tau_\beta)$. Here $F(S', \tau)$ is a linear weighted sum of the form

TABLE II. Absolute values of the coefficients of nonlinear cardiorespiratory interactions corresponding to the last three base functions in (3), $\{x_r x_c, x_r^2 x_c, x_r x_c^2\}$. Coefficients $\{\alpha_i\}$ correspond to the respiration coupling to cardiac rhythm. Coefficients $\{\beta_i\}$ correspond to the cardiac oscillation coupling to respiration. For each set of coefficients the actual values (top row) are compared to the mean inferred values obtained from 100 nonoverlapped 1600 s blocks of data $\{x_r(t), x_c(t), y_r(t), y_c(t)\}$. Each block includes 160 000 points with a sampling time of 0.01 s (middle row). The estimation error is shown in the bottom line.

α_{20}	β_{20}	α_{21}	β_{21}	α_{22}	β_{22}	D_{11}	D_{22}
0.12	2.20	0.048	0.27	−0.066	−8.67	0.18	8.13
0.12	2.41	0.048	0.28	−0.070	−8.61	0.18	8.14
2.9%	9.3%	1.8%	5.6%	5.2%	0.7%	0.2%	0.2%

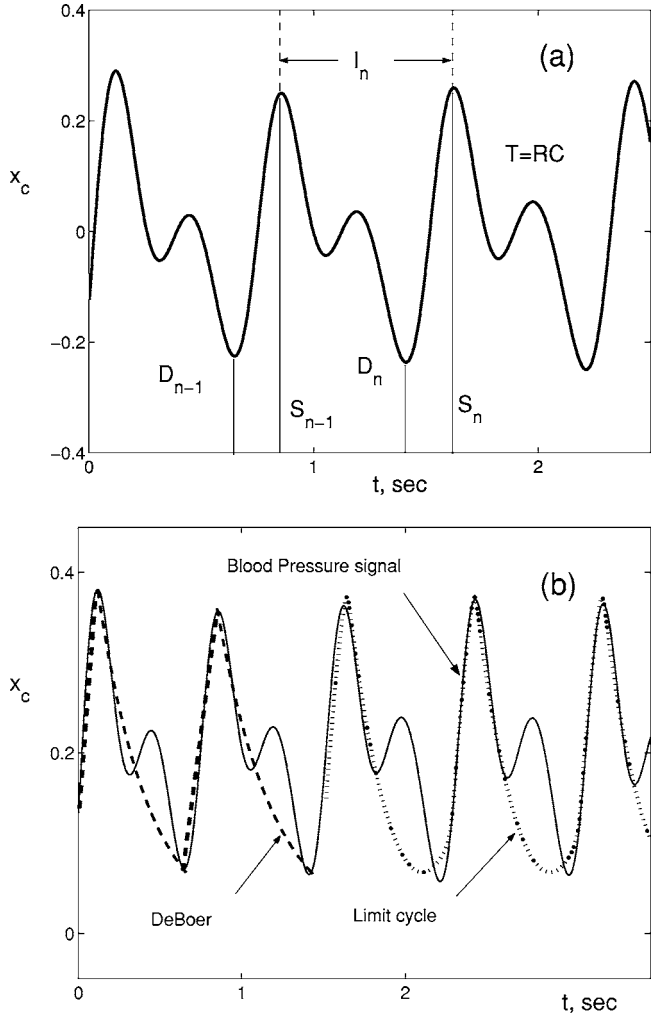

FIG. 7. (a) The BP signal in the frequency range of cardiac oscillations (black line). Systolic pressure (S_n), diastolic pressure (D_n), RR intervals (I_n), and arterial decay time ($T=RC=1{,}318$ ms) are shown for the nth heartbeat. (b) Comparison of the BP signal (thin black line) with the approximations adopted in the DeBoer (dashed line) and FitzHugh-Nagumo (dotted line) models. The vertical scale has arbitrary units.

$$F(S',\tau)=\sum_{k=-M}^{M} a_k S'_{i-\tau+k} = \frac{(S'_{i-\tau-2}+2S'_{i-\tau-1})+(3S'_{i-\tau}+2S'_{i-\tau+1}+S'_{i-\tau+2})}{9}$$

Furthermore, we assume for simplicity that the pressure oscillations do not deviate far from the working point S_0 in (22), i.e., $S' \approx S$.

To establish the connection between the DeBoer model (19)–(21) and the model (1),(2) presented in this paper, we note that the DeBoer model is a piecewise approximation of the actual BP signal. In particular, it describes the BP signal as an exponential decay during 2/3 of the *RR* interval and a linear increase during 1/3 of the I_n as shown in Fig. 7(b). We also note that this model of cardiac oscillations (2) resembles the FitzHugh-Nagumo (FHN) model of the system

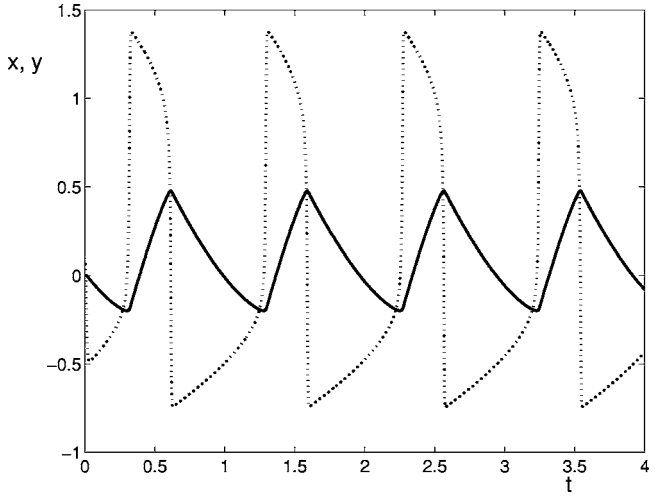

FIG. 8. Time evolution of the dynamical variables x (solid line) and y (dashed line) of the FHN system with parameters: $\epsilon=0.01$, $\beta=-0.05$, $C=-0.125$, $\alpha=0.5$, $\gamma=1$, $\delta=-1$.

$$\begin{cases} \dot{x}=\epsilon(y-\beta x), \\ \dot{y}=\alpha y+\gamma y^2+\delta y^3-x+C, \end{cases} \tag{23}$$

where we have neglected for a moment the cardiorespiratory interaction. The approximation of the BP signal by the output of the FHN system is also shown in Fig. 7(b). It can be seen already from a comparison between the two approximations that there is a close connection between the DeBoer model and the model of coupled oscillators considered in this paper. This can be further illustrated by noting that for small ϵ the limit cycle in the FHN system consists of fast motion with practically constant values of y, when y jumps between negative and positive values, and slow motion, when y changes very little (see Fig. 8). Assuming a constant value of y at the top $|a_+|$ and at the bottom $-|a_-|$ of the dashed curve corresponding to slow motion along the limit cycle, we can integrate the first equation in (23) to obtain

$$x_0(t)=\begin{cases} \left(S_{n-1}+\dfrac{|a_-|}{\beta}\right)e^{-\beta t}-\dfrac{|a_-|}{\beta}, & \text{for } 0<t<\dfrac{2}{3}I_n; \\ \left(D_n-\dfrac{|a_+|}{\beta}\right)e^{-\beta t}+\dfrac{|a_+|}{\beta}, & \text{for } \dfrac{2}{3}I_n<t<I_n. \end{cases}$$

This solution closely resembles Eqs. (19) and (20) of the DeBoer model.

It can be seen even from this simplified discussion that the parameters of the model (1) and (2) found in the present paper can be related directly to the physiological parameters of the autonomous control of circulation. Furthermore, this discussion suggests that it should be possible at least, in principle, to bridge inverse and forward modeling and to infer parameters of the autonomous nervous control of the cardiovascular system directly from the time-series data.

We emphasize, however, that the results obtained represent only a first step in this direction. In particular, the DeBoer model itself has to be modified in various ways, including more realistic functional form of the feedback terms and specifically so as to take into account the fact that the barore-

flex control is a closed loop [18,20]. In fact, it was shown [73] that a multicompartment closed-loop model of the cardiovascular responses can simulate well the experimentally observed variations in the time series. On the other hand, this comparison suggests that the inference scheme used in this paper has to be modified in various ways to facilitate convergence and guarantee deeper physiological meaning of the model parameters, as will be discussed in more detail elsewhere. It is also important to emphasize that dynamical inference of more sophisticated multidimensional models of the type [73], as well as coupled oscillatory models [13], can now be addressed within the framework of full Bayesian inference of the unknown dynamical variables.

VII. CONCLUSION

In the present paper we have presented a technique for nonlinear dynamical inference of cardiovascular interactions from blood pressure time-series data. The method is applied to the simultaneous estimation of the dynamical couplings and noise strengths in a model of the nonlinear cardiorespiratory interaction. We have identified a simple nonlinear stochastic dynamical model of the cardiorespiratory interaction that describes, within the framework of inverse modeling, the time-series data in a particular frequency band. The method was validated by use of synthesized data obtained by numerically integrating the inferred model itself. We have shown that main source of error in the method is the decomposition of the blood pressure signal into two oscillatory components. We illustrate in the discussion that the dynamical model of the cardiorespiratory interaction identified in the present research can be related to the well-known beat-to-beat model of cardiovascular control by DeBoer *et al.* [68]. The method developed in this paper can be used to infer the parameters of stochastic nonlinear dynamical models from observed phenomena and is applicable across many scientific disciplines.

ACKNOWLEDGMENTS

This work was supported by the Engineering and Physical Science Research Council (UK), NASA CICT-IS-DU Project (USA), the Russian Foundation Science, Wellcome Trust, the ARRS (Slovenia), and INTAS.

[1] R. D. Berger, J. P. Saul, and R. J. Cohen, Am. J. Physiol. Heart Circ. Physiol. **256**, H142 (1989).
[2] L. P. Faucheux, L. S. Bourdieu, P. D. Kaplan, and A. J. Libchaber, Phys. Rev. Lett. **74**, 1504 (1995).
[3] T. J. Mullen *et al.*, Am. J. Physiol. Heart Circ. Physiol. **272**, H448 (1997).
[4] R. Mukkamala *et al.*, Am. J Physiol.: Regul. Integr. Compar. Physiol. **276**, R905 (1999).
[5] R. Mukkamala and R. J. Cohen, Am. J. Physiol. Heart Circ. Physiol. **281**, H2714 (2001).
[6] G. Nollo *et al.*, Am. J. Physiol. Heart Circ. Physiol. **280**, H1830 (2001).
[7] K. H. Chon, T. J. Mullen, and R. J. Cohen, IEEE Trans. Biomed. Eng. **43**, 530 (1996).
[8] S. Lu and K. H. Chon, IEEE Trans. Signal Process. **51**, 3020 (2003).
[9] D. Jordan, in *Cardiovascular regulation*, edited by D. Jordan and J. Marshall (Portland Press, Cambridge, 1995).
[10] H. Seidel and H. Herzel, in *Modeling the Dynamics of Biological Systems*, edited by E. Mosekilde and O. G. Mouritsen (Springer, Berlin, 1995), pp. 205–229.
[11] H. Seidel and H. Herzel, Physica D **115**, 145 (1998).
[12] G. G. Berntson *et al.*, Psychophysiology **34**, 623 (1997).
[13] A. Stefanovska and M. Bračič, Contemp. Phys. **40**, 31 (1999).
[14] S. C. Malpas, Am. J. Physiol. Heart Circ. Physiol. **282**, H6 (2002).
[15] I. Majercak, Bratisl Lek Listy **103**, 368 (2002).
[16] P. V. E. McClintock, and A. Stefanovska, in *Fluctuations and Noise in Biological, Biophysical and Biomedical Systems II*, edited by D. Abbott, S. M. Bezrukov, A. Der, and A. Sanchez (SPIE, Bellingham, WA, 2004), pp. 54–68.
[17] S. Eyal and S. Akselrod, Methods Inf. Med. **39**, 118 (2000).
[18] T. Sato *et al.*, Am. J. Physiol. Heart Circ. Physiol. **276**, H2251 (1999).
[19] P. van Leeuwen and H. Bettermann, Herzschr Elektrophys **11**, 127 (2000).
[20] J. V. Ringwood and S. C. Malpas, Am. J. Physiol.: Reg. Integr. Compar. Physiol. **280**, R1105 (2001).
[21] A. Stefanovska, D. G. Luchinsky, and P. V. E. McClintock, Physiol. Meas **22**, 551 (2001).
[22] K. Kotani, K. Takamasu, Y. Ashkenazy, H. E. Stanley, and Y. Yamamoto, Phys. Rev. E **65**, 051923 (2002).
[23] J. A. Taylor *et al.*, Am. J. Physiol. Heart Circ. Physiol. **280**, H2804 (2001).
[24] R. Zou and K. H. Chon, IEEE Trans. Biomed. Eng. **51**, 219 (2004).
[25] J. A. Taylor *et al.*, Am. J. Physiol. Heart Circ. Physiol. **280**, H2804 (2001).
[26] K. H. Chon, IEEE Trans. Biomed. Eng. **48**, 622 (2001).
[27] J. Jamšek, A. Stefanovska, P. V. E. McClintock, and I. A. Khovanov, Phys. Rev. E **68**, 016201 (2003).
[28] J. Jamšek, A. Stefanovska, and P. V. E. McClintock, Phys. Med. Biol. **49**, 4407 (2004).
[29] M. G. Rosenblum, L. Cimponeriu, A. Bezerianos, A. Patzak, and R. Mrowka, Phys. Rev. E **65**, 041909 (2002).
[30] M. Paluš, V. Komárek, Z. Hrnčíř, and K. Štěbrová, Phys. Rev. E **63**, 046211 (2001).
[31] R. Mrowka, L. Cimponeriu, A. Patzak, and M. G. Rosenblum, Am. J. Physiol.: Regul. Integr. Compar. Physiol. **285**, R1395 (2003).
[32] C. Schäfer, M. G. Rosenblum, J. Kurths, and H. H. Abel, Nature (London) **392**, 239 (1998).
[33] N. B. Janson, A. G. Balanov, V. S. Anishchenko, and P. V. E. McClintock, Phys. Rev. Lett. **86**, 1749 (2001).
[34] N. B. Janson, A. G. Balanov, V. S. Anishchenko, and P. V. E. McClintock, Phys. Rev. E **65**, 036212 (2002).

[35] S. Lu, H. Ju, and K. H. Chon, IEEE Trans. Biomed. Eng. **48**, 1116 (2001).
[36] R. Meyer and N. Christensen, Phys. Rev. E **65**, 016206 (2001).
[37] P. E. McSharry and L. A. Smith, Phys. Rev. Lett. **83**, 4285 (1999).
[38] J. P. M. Heald and J. Stark, Phys. Rev. Lett. **84**, 2366 (2000).
[39] R. Meyer and N. Christensen, Phys. Rev. E **62**, 3535 (2000).
[40] J.-M. Fullana and M. Rossi, Phys. Rev. E **65**, 031107 (2002).
[41] S. Siegert, R. Friedrich, and J. Peinke, Phys. Lett. A **253**, 275 (1998).
[42] M. Siefert, A. Kittel, R. Friedrich, and J. Peinke, Europhys. Lett. **61**, 466 (2003).
[43] J.-M. Fullana and M. Rossi, Phys. Rev. E **65**, 031107 (2002).
[44] V. N. Smelyanskiy, D. G. Luchinsky, D. A. Timuçin, A. Bandrivskyy, and D. G. Luchinsky, Phys. Rev. E **72**, 026202 (2005).
[45] M. B. Willemsen, M. P. van Exter, and J. P. Woerdman, Phys. Rev. Lett. **84**, 4337 (2000).
[46] K. Visscher, M. J. Schnitzer, and S. M. Block, Nature (London) **400**, 184 (1999).
[47] D. J. D. Earn, S. A. Levin, and P. Rohani, Science **290**, 1360 (2000).
[48] J. Christensen-Dalsgaard, Rev. Mod. Phys. **74**, 1073 (2002).
[49] V. N. Smelyanskiy, D. G. Luchinsky, A. Stefanovska, and P. V. E. McClintock, Phys. Rev. Lett. **94**, 098101 (2005).
[50] P. J. Saul, D. T. Kaplan, and R. I. Kitney, in *Computers in Cardiology* (IEEE Comput. Soc. Press, Washington, 1989), pp. 299–302.
[51] A. Stefanovska, M. Bračič, S. Strle, and H. Haken, Physiol. Meas **22**, 535 (2001).
[52] A. Stefanovska and P. Krošelj, Open Syst. Inf. Dyn. **4**, 457 (1997).
[53] A. J. Camm, M. Malik, J. T. Bigger *et al.*, Circulation **93**, 1043 (1996).
[54] A. J. Taylor, D. L. Carr, C. W. Myers, and D. L. Eckberg, Circulation **98**, 547 (1998).
[55] M. W. R. Milnor, *Hemodynamics* (Williams and Wilkins, Baltimore, 1989).
[56] I. Javorka, M. ans Zila, K. Javorka, and A. Calkovska, Physiol. Rev. **51**, 227 (2002).
[57] R. W. DeBoer, J. M. Karemaker, and J. Strackee, Am. J. Physiol. **253**, H680 (1987).
[58] E. W. Taylor, D. Jordan, and J. H. Coote, Physiol. Rev. **79**, 855 (1999).
[59] H. P. Koepchen, in *Mechanisms of Blood Pressure Waves*, edited by K. Miyakawa, H. P. Koepchen, and C. Polosa (Springer, Berlin, 1984).
[60] A. Melcher, Acta Physiol. Scand. Suppl. **435**, 1 (1976).
[61] F. L. Abel and J. A. Waldhausen, Am. Heart J. **78**, 266 (1969).
[62] M. P. Gilbey, D. Jordan, D. W. Richter, and K. M. Spyer, J. Physiol. (London) **365**, 67 (1984).
[63] L. Glass and M. C. Mackey, *From Clocks to Chaos* (Princeton University Press, Princeton, 1988).
[64] C. Braun *et al.*, Am. J. Physiol. Heart Circ. Physiol. **275**, H1577 (1998).
[65] K. Suder, F. R. Drepper, M. Schiek, and H.-H. Abel, Am. J. Physiol. Heart Circ. Physiol. **275**, H1092 (1998).
[66] V. Novak *et al.*, J. Appl. Physiol. **74**, 617 (1993).
[67] J. K. Kanters, M. V. Hojgaard, E. Agner, and N. H. Holstein-Rathlou, Am. J. Physiol. **272**, R1149 (1997).
[68] R. W. de Boer, J. M. Karemaker, and J. Strackee, Psychophysiology **22**, 147 (1985).
[69] D. K. Arrowsmith and C. M. Place, *Ordinary Differential Equations* (Chapman and Hall, London, 1982).
[70] R. Meyer and N. Christensen, Phys. Rev. E **62**, 3535 (2000).
[71] R. Graham, Z. Phys. B **26**, 281 (1977).
[72] M. I. Dykman, Phys. Rev. A **42**, 2020 (1990).
[73] T. Heldt, E. B. Shim, R. D. Kamm, and R. G. Mark, J. Appl. Physiol. **92**, 1239 (2002).